

1

2 ~~Antarctic Peninsula ice shelf collapse triggered by föhn~~

3 ~~wind-induced melt~~

4 **The role of föhn winds in Antarctic Peninsula rapid ice shelf collapse**

5 Matthew K. Laffin¹, Charles S. Zender^{1,2}, Melchior van Wessem³, Sebastián Marinsek⁴

6 ¹Department of Earth System Science, University of California, Irvine

7 ²Department of Computer Science, University of California, Irvine

8 ³Institute for Marine and Atmospheric Research Utrecht (IMAU), Utrecht University

9 ⁴Instituto Antártico Argentino, Buenos Aires, Argentina

10 *Correspondence to:* Matthew K. Laffin (mlaffin@uci.edu)

11 **Abstract.** Ice shelf collapse reduces buttressing and enables grounded glaciers to contribute more rapidly to sea-level rise in
12 a warming climate. The abrupt collapses of the Larsen A (1995) and B (2002) ice shelves on the Antarctic Peninsula (AP)
13 ~~have been attributed to increased surface melt~~ occurred while large period ocean swells damaged the calving fronts and the
14 ice shelves were inundated with melt lakes that led to large-scale hydrofracture cascades. During collapse, surface
15 observations indicate föhn winds were present on both ice shelves. ~~However, no studies examine the timing, magnitude, and~~
16 ~~location of surface melt processes immediately preceding these disintegrations.~~ Here we use a regional climate model and
17 Machine Learning analyses to evaluate the contributory ~~influence~~ roles of föhn winds and associated melt ~~events~~ events prior
18 to and during the collapses for ice shelves on the AP. ~~on the surface liquid water budget for collapsed and extant ice~~
19 ~~shelves. We find~~ Föhn winds caused about $25\% \pm 3\%$ of the total annual melt in just 9 days on Larsen A- prior to and during
20 collapse and were present during the Larsen B collapse which helped form extensive melt lakes that surpassed a critical
21 stability depth ~~that, we suggest, ultimately triggered collapse. By contrast, föhns appear to pre-condition~~. At the same time
22 the off-coast wind direction created by föhn winds helped melt and physically push sea ice away from the ice shelf calving
23 fronts that allowed large period ocean swells to reach and damage the front, which ultimately triggered collapse. ~~not trigger,~~
24 ~~Larsen B's collapse.~~ Collapsed ice shelves experienced enhanced surface melt driven by föhn winds over a large spatial
25 extent and near the calving front, ~~wh~~ AP areas extant ice shelves are affected less by föhn wind-induced melt and do not
26 experience regular melt ponds. These results suggest extant ice shelves ~~will remain less vulnerable to~~ are less likely to
27 experience rapid collapse ~~surface-melt-driven instability~~ due to ~~weaker~~ föhn-driven melt so long as surface temperatures and
28 föhn occurrence remain within historical bounds.

29 **1 Introduction**

30 The sudden disintegration of ice shelves on the eastern periphery of the Antarctic Peninsula (AP) represents the culmination
31 of a critical regional ~~warming trend and anomalous surface melt in the region (Vaughan et al., 2003). Forensic examination~~
32 ~~of surface melt on ice shelves, which subdue the discharge of~~arming trend and anomalous surface melt in the region
33 (Vaughan et al., 2003). Ice shelves, the floating extensions of grounded glaciers, subdue the discharge of grounded ice into
34 the global ocean (Rignot et al., 2004; Scambos et al., 2004; Gudmundsson et al., 2013; Borstad et al., 2016). Re-examination
35 of past ice shelf collapse events ~~grounded ice into the global ocean,~~can help to shed light on the mechanisms of collapse ~~can~~
36 ~~lead to~~and improved the understanding of ice shelf dynamics for future projections of sea-level rise (Rignot et al., 2004;
37 Gudmundsson et al., 2013; Borstad et al., 2016). The final collapses of the Larsen A (LAIS) in 1995 and the Larsen B
38 (LBIS) ice shelves in 2002 have been attributed to decreased structural integrity brought on by a combination of factors.
39 Most notably, regional atmospheric warming (Scambos et al., 2000; Mulvaney et al., 2012), extended melt seasons (Scambos
40 et al., 2003), multi-year firm pore space depletion (Kuipers Munneke et al., 2014; Trusel et al., 2015), melt pond flooding and
41 crevasse expansion through hydrofracture (Scambos et al., 2003; Trusel et al., 2013; Pollard et al., 2015; Alley et al., 2018;
42 Banwell et al., 2019; Robel and Banwell, 2019; Leeson et al., 2020), glacier structural discontinuities (Glasser et al., 2008),
43 basal melt (Pritchard et al., 2012; Rignot et al., 2013; Depoorter et al., 2013; Schodlok et al., 2016; Adusumilli et al., 2018),
44 warm melt-water intrusion (Braun et al., 2009), melting of the ice melange within rifts conducive to rift propagation (Larour
45 et al., 2021), and regional sea ice loss allowing ocean swell flexure stress on the calving front (Banwell et al., 2017; Massom
46 et al., 2018).

47 While the list of mechanisms that can destabilise ice shelves is extensive, a conceptual model for rapid ice shelf
48 collapse proposed by Massom et al., (2018) identifies 4 essential prerequisites for sudden collapse: (1) extensive surface
49 flooding and hydrofracture; (2) reduced sea ice or fast ice at the ice shelf front; (3) outer margin or terminus fracturing and
50 rifting; and (4) initial calving trigger at the ice shelf margin. In addition Massom et al., (2018) concluded that a lack of
51 summer sea ice allowed large period ocean swells to reach the ice shelf calving front. They theorise waves led to calving
52 front damage and small calving events that breached the “compressive arch” of stability of both ice shelves proposed by
53 Doake et al., (1998). At the same time the ice shelves were covered in extensive surface melt lakes that were unlikely to
54 drain horizontally because of the relatively flat surface (Banwell et al., 2014). Satellite observations and ice shelf stability
55 model studies determined the LBIS was covered with >2750 melt lakes that were on average 1 meter deep before collapse
56 which corresponds to a possible melt lake depth stability threshold for ice shelves in the region (Glasser and Scambos
57 (2008); Banwell et al., 2013). Ice shelves inundated with surface melt lakes are susceptible to disintegration through a
58 process known as hydrofracture, where meltwater applies outward and downward pressure to the walls and tip of crevasses

59 that can propagate through the ice shelf (Scambos et al., 2003; Banwell et al., 2013; Bell et al., 2018; Lhermitte et al., 2020).
60 Furthermore, melt lakes at critical water depths can create fracture patterns that split ice shelves into sections with aspect
61 ratios that support unstable rollover, and hydrofracture cascades that begin when melt lakes drain and/or calving occurs at the
62 ice shelf terminus (Scambos et al., 2003; Banwell et al., 2013; Burton et al., 2013; Robel and Banwell (2019)). The
63 combination of ocean swell stress on the calving front and extensive melt ponds led to large scale hydrofracture cascades that
64 proposed by Massome et al., (2018) ultimately caused the rapid collapse of LAIS and LBIS.

65 In addition to a lack of sea ice and extensive melt ponds, meteorological and satellite observations identify clear
66 skies and warm west/northwest föhn wind at the time of collapse (Figure 1b-f) (Rott et al., 1998; Rack and Rott (2004); Cape
67 et al., 2015; Massom et al., 2018). Föhn winds form when relatively cool moist air is forced over a mountain barrier, often
68 leading to precipitation on the windward side of the barrier that dries the air mass (Grosvenor et al., 2014; Elvidge et al.,
69 2015). As the now drier air descends the leeward slope it warms adiabatically and promotes melt directly through sensible
70 heat exchange, and indirectly by the associated clear skies that allow additional shortwave radiation to reach the surface in
71 non-winter months (Turton et al., 2017, 2018; Kuipers Munneke et al., 2018; Elvidge et al., 2020; Laffin et al., 2021). Föhn
72 winds and their capacity to cause surface melt have been studied extensively on the AP. Observations and model studies on
73 the LCIS confirm the föhn mechanism that enhances sensible heat and shortwave radiation and alters local albedo which can
74 increase surface melt rates upwards of 50% compared to non-föhn conditions (Cape et al., 2015; Elvidge et al., 2015; King et
75 al., 2015, 2017; Kuipers Munneke et al., 2012, 2018; Bevan et al., 2017; Lenaerts et al., 2017; Datta et al., 2019;
76 Kirchgaessner, et al., 2021; Laffin et al., 2021, Wang et al., 2021). Late season föhn melt reduces firn pore space, and thus
77 pre-conditions ice shelves to form melt ponds and are responsible for the increased firn density pattern east of the AP
78 mountains on the LCIS (Holland et al., 2011; Kuipers Munneke et al., 2014; Datta et al., 2019). Föhn melt climatology
79 studies have aimed to identify how much melt is caused by föhn and the locations most affected and found föhn winds
80 account for up to 17 % of melt and are concentrated in the LCIS inlets (Turton et al., 2017; Datta et al., 2019; Laffin et al.,
81 2021). Pressure gradient differences across the AP range lead to föhn winds that funnel through mountain gaps as highly
82 concentrated föhn jets, particularly in inlets east of the AP range (Luckman et al., 2014; Elvidge et al., 2015; Kuipers
83 Munneke et al., 2012; Grosvenor et al., 2014). In addition to enhancing surface melt rates, föhn winds exert force on sea/fast
84 ice and drag it away from the calving front, thereby exposing the front to ocean waves (Bozkurt et al., 2018). Climatic
85 studies of the Larsen B embayment indicate that föhn winds were coincident with collapse (Rack and Rott (2004); Leeson et
86 al., 2017). However, it is unknown if concentrated föhn jets spilled onto the former LAIS and LBIS and, if so, whether those
87 föhn winds contributed to their collapse. The questions, therefore, arise: 1) To what extent does föhn-induced melt contribute
88 to the surface melt budget on the AP, specifically LAIS and LBIS?; 2) Did föhn winds and associated melt play a role in
89 triggering the collapses of the LAIS and LBIS?; 3) What are the implications of föhn-induced melt for the remaining eastern
90 AP ice shelves?

91 To address these questions we consider three metrics: Section 3.1 explores the total annual surface melt quantity induced by
92 föhn winds and how melt is spatially distributed across each ice shelf; Section 3.2 identifies the coincidence of föhn-induced
93 melt preceding and during the collapse events, and the estimated melt-lake depth in response to melt events.; Section 3.3
94 identifies the contribution of föhn melt to the climatological surface liquid water budget comparing collapsed and extant ice
95 shelves. By constructing a timeline of melt and melt mechanisms and comparing melt metrics with collapsed and extant ice
96 shelves, we can identify the contributory factors to collapse. Enhanced regional temperatures and associated surface
97 meltwater are considered the leading contributors to the final stages of the Larsen A and B ice shelf collapses (Van Den
98 Broeke et al., 2005; Trusel et al., 2013), and have received considerable scientific attention, but the detailed mechanisms that
99 melt the surface, and the rate and timing of surface melt, particularly föhn wind-induced have not been examined in
100 complete detail. Here, using Machine Learning (ML) methods to identify föhn events we document the existence of strong
101 föhn jets and increased surface melt rates preceding the final collapse events and assess the significance of the föhn-melt
102 mechanism for the stability of the remaining eastern AP ice shelves. Our ML method is the most accurate method to identify
103 föhn winds, and when combined with regional climate model output produces the most accurate melt mechanism
104 quantification.

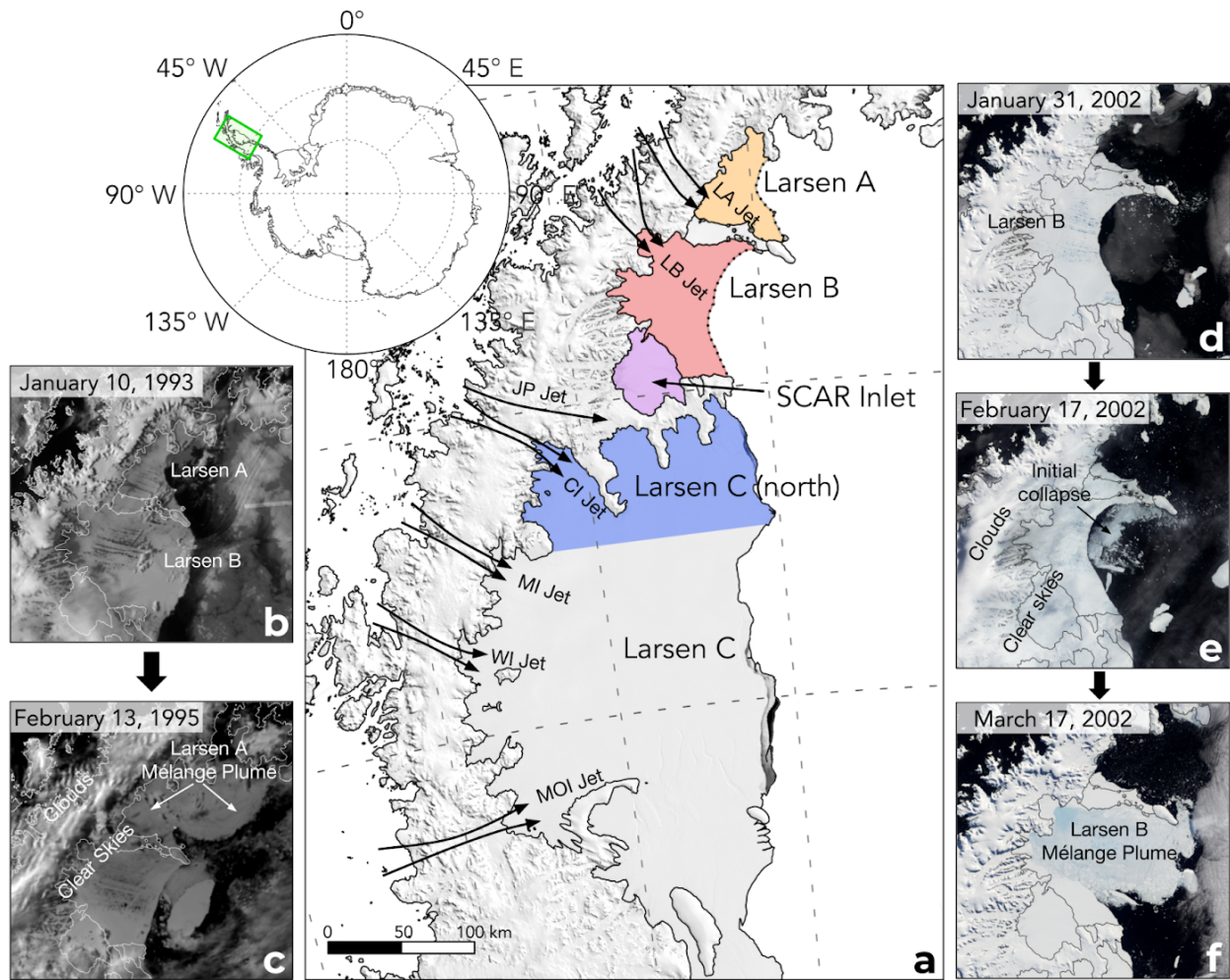
105 The final collapses of the Larsen A (LAIS) in 1995 and the Larsen B (LBIS) ice shelves in 2002 have been
106 attributed to decreased structural integrity brought on by a combination of factors. Most notably, regional atmospheric
107 warming (Seambos et al., 2000; Mulvaney et al., 2012), extended melt seasons (Seambos et al., 2003), multi-year firn pore
108 space depletion (Kuipers Munneke et al., 2012; Trusel et al., 2015), melt pond flooding and crevasse expansion through
109 hydrofracture (Seambos et al., 2003; Pollard et al., 2015; Banwell et al., 2019; Robel and Banwell, 2019), glacier structural
110 discontinuities (Glasser et al., 2008), basal melt (Pritchard et al., 2012; Rignot et al., 2013; Depoorter et al., 2013; Schodlok
111 et al., 2016; Adusumilli et al., 2016), warm melt-water intrusion (Braun et al., 2009), melting of the ice mélange within rifts
112 conducive to rift propagation (Poinelli et al., 2021), and regional sea ice loss allowing ocean swell flexure stress on the
113 calving front (Massom et al., 2018). Satellite observations and ice shelf stability model studies have determined the LBIS
114 was covered with >2750 melt lakes that were on average 1 meter deep before collapse which corresponds to a possible melt
115 lake depth of stability threshold for ice shelves in the region (Glasser et al., 2008; Banwell et al., 2013). Ice shelves
116 inundated with surface melt lakes are susceptible to disintegration through a process known as hydrofracture, where
117 meltwater applies outward and downward pressure to the walls and tip of crevasses that can propagate through the ice shelf
118 (Seambos et al., 2003; Banwell et al., 2013; Bell et al., 2018). Melt lakes at critical water depths create a fracture pattern that
119 splits ice shelves into sections with aspect ratios that support unstable rollover and hydrofracture cascades that begin when
120 melt lakes drain or calving occurs at the ice shelf terminus (Banwell et al., 2013; Robel et al., 2019).

121 Previous research acknowledges enhanced surface melt during years of collapse and the presence of föhn wind
122 events in the region, however, no attempt to produce a timeline of total melt quantity or melt caused by föhn before and

123 ~~during ice shelf breakup has been undertaken. Before and during the final stage of the collapse events, satellite observations~~
124 ~~indicate numerous surface melt lakes and a sky generally clear of clouds (Figure 1b-f). Clear skies are one indicator that high~~
125 ~~melt rate northwesterly downslope föhn winds may have been present during the collapse events (Elvidge et al., 2020; Laffin~~
126 ~~et al., 2021). Although the AP is one of the fastest-warming regions on Earth there have been no additional sudden collapse~~
127 ~~events on the eastern AP since 2002 (Vaughan et al., 2003; Bozkurt et al., 2020). The questions, therefore, arise: 1) To what~~
128 ~~extent does föhn-induced melt contribute to the surface melt budget on the AP?; 2) Does the confluence of föhn-induced~~
129 ~~melt quantity, spatial impact, and timing constitute a trigger for the collapse of the LAIS and LBIS?; 3) What are the~~
130 ~~implications of föhn-induced melt for the remaining eastern AP ice shelves?~~

131 ~~To address these questions we consider three metrics: Section 3.1 explores the total annual melt quantity and spatial~~
132 ~~distribution caused by föhn winds.; Section 3.2 identifies the coincidence of föhn-induced melt preceding and during the~~
133 ~~collapse events, and the estimated melt lake depth in response to melt events.; Section 3.3 identifies the contribution of föhn~~
134 ~~melt to the climatological surface liquid water budget comparing collapsed and extant ice shelves. By constructing a timeline~~
135 ~~of melt and melt mechanisms and comparing melt metrics with collapsed and extant ice shelves, we can identify the~~
136 ~~contributing factors that caused collapse.~~

137



138 **Figure 1.** Map of the northern Antarctic Peninsula (a) showing locations of ice shelves and föhn jets (Larsen A jet (LA jet), Larsen B jet
 139 (LB jet), Jason Peninsula jet (JP jet), Cabinet inlet jet (CI jet), Mill inlet jet (MI jet), Whirlwind inlet jet (WI jet), Mobil Oil inlet jet (MOI
 140 jet)) with a MODIS Mosaic overlay. The colored regions indicate how this study separates ice shelves for climatic analysis. The dotted
 141 lines show the former extent of the Larsen A and Larsen B ice shelves at the time of collapse. Panels (b)-(f) are satellite images of the
 142 collapses of the LAIS and LBIS. (b) AVHRR (Advanced Very High-Resolution Radiometer) image of the northern AP two years before
 143 the collapse of the LAIS showing melt lakes on the surface of both ice shelves. (c) AVHRR image after the collapse of the LAIS. (d)
 144 MODIS (Moderate Resolution Imaging Spectroradiometer) image showing the LBIS days before collapse began. (e) MODIS image
 145 showing a föhn wind event (clouds over the western AP, clear skies over the ice shelves) along with the initial collapse of the LBIS. (f)
 146 MODIS image of the complete collapse of the LBIS.

147 2 Data and methods

148 2.1 Regional Climate Model ~~Data~~ Simulation (RACMO2)

149 We base our analysis on 3-hourly output from simulations by the Regional Atmospheric Climate Model 2 (RACMO2),
150 version 2.3p2, with a horizontal resolution of 5.5km (0.05°) focused on the AP from 1979-2018. RACMO2 uses the physics
151 package CY33r1 of the ECMWF Integrated Forecast System (IFS)
152 (<https://www.ecmwf.int/en/elibrary/9227-part-iv-physical-processes>\textit{{ECMWF-IFS,} 2008}) in combination with
153 atmospheric dynamics of the High-Resolution Limited Area Model (HIRLAM). RACMO2 has been evaluated against
154 numerous surface observations (~~AWS~~) in locations all over the AP and has trouble simulating very high and low-temperature
155 extremes in the region but is considered a good representation of surface conditions (Leeson et al., 2017; Laffin et al., 2021).

156 2.2 Föhn wind detection

157 We ~~developed~~ use the Föhn Detection Algorithm (FöhnDA) that identifies föhn winds that cause melt using 12 Automatic
158 Weather Stations (AWS) on the AP ~~as~~ previously developed and detailed in Laffin et al., (2021). FöhnDA identifies
159 föhn-induced melt events using binary classification Machine Learning when 10 metre air temperature (T) is greater than
160 0°C, which ensures it captures föhn events that cause surface melt. ~~-~~Thresholds for relative humidity (RH) and wind speed
161 (WS) are more dynamic because high wind speeds and low relative humidity do not guarantee temperatures above freezing,
162 they only aid to identify föhn. FöhnDA uses quantile regression to identify these variable thresholds that take into account
163 the climatology and seasonality at each ~~weather station~~ AWS site. FöhnDA uses two empirically determined thresholds: the
164 60th percentile wind speed and 30th percentile relative humidity which are 2.85 m/s and 79% averaged at all AWS
165 locations. We co-locate AWS with the nearest model grid cell and use FöhnDA results to train an ML model that detects
166 föhn winds in RACMO2 output. Our ML model improves the accuracy of föhn detection by over 23% when compared to the
167 simple binary classification method applied to RACMO2 output as described above. A sensitivity study detailed in Laffin et
168 al., (2021) compares previous föhn detection methods (Cape et al., 2015; Datta et al., 2019) and shows ~~that this method~~
169 FöhnDA is the most accurate detection method ~~compared to previous work~~ and allows us to use in situ observations from
170 AWS and expand föhn detection with RACMO2 output to regions and times when AWS observations are not available
171 (Figure S21) (Table S1).

172 Föhn jet locations were identified using wind direction and strength during föhn events (Figure 2a) and by the
173 surface melt pattern during föhn (Figure 3b). The RACMO2 topography pixel size is 5.5 km which is sufficient to produce
174 the föhn jets identified on the LCIS (Elvidge et al., 2015), and allows for new föhn jet identification on the LAIS and LBIS
175 despite lack of direct observation. ~~-~~ However, small-scale föhn winds ~~funneled~~ funnelled through local canyons and mountain

176 gaps smaller than 5.5 km are not directly simulated. Therefore, we consider RACMO2 simulated estimates of surface melt
177 caused by föhn winds to be conservative and likely higher in regions where föhn winds are funneled and
178 concentrated.

179 2.3 Ice shelf intercomparison analysis

180 We split each of the five ice shelves into areas shown in Figure 1a (Larsen A, Larsen B, SCAR inlet, Larsen C (north),
181 and Larsen C) and take the average of all model grid cells annually to create a climatology of surface melt, melt rate, melt
182 hours, surface temperature. We use a two-tailed t-test statistic to identify if the mean surface temperature and mean surface
183 melt of both ice shelves are statistically different from one another at the 95% confidence interval. We compare all ice
184 shelves to the LBIS because it was the most recent collapse event and is adjacent to collapsed and existing ice shelves.
185 Qualitatively similar results are obtained when comparing all ice shelves to the LAIS.

186 To compare ice shelf liquid water budgets we use a liquid-to-solid ratio (LSR) as a crude proxy for available firm air
187 content and can be estimated as,

$$189 \quad LSR = \frac{\text{Total liquid water (snowmelt + liquid precipitation)}}{\text{Total solid precipitation (snow)}} \quad (1)$$

190
191 where areas with $LSR < 1$ represent an ice shelf that receives more solid precipitation than liquid water and is therefore less
192 likely to saturate with liquid water and form melt lakes than areas with $LSR > 1$.

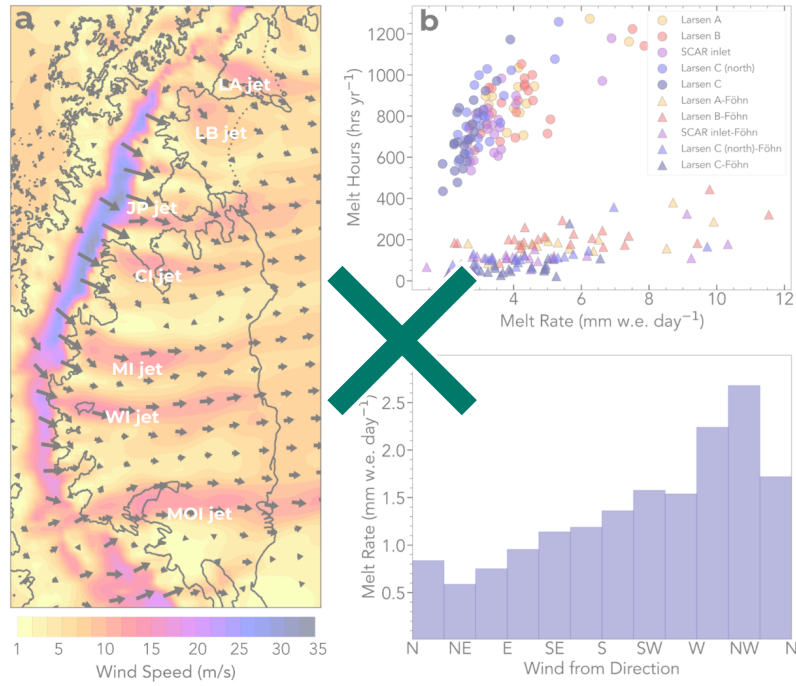
193 3 Results

194 3.1 Föhn jets and melt

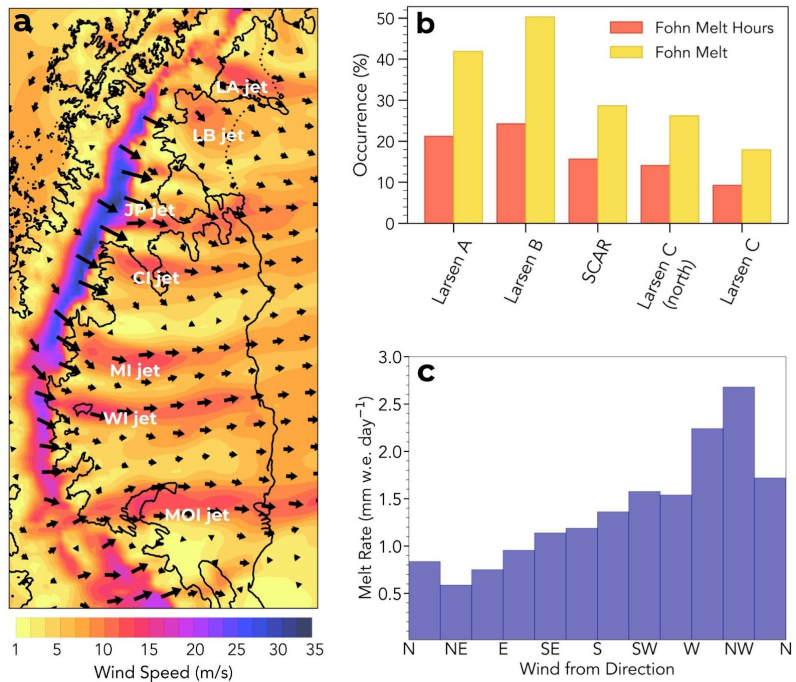
195 Using RACMO2 historical simulations, informed by a Machine Learning algorithm that is trained with Automatic Weather
196 Station (AWS) observations (Laffin et al., 2021), we identify seven recurring föhn jets or “gap winds” that lead to high
197 surface melt rates on the eastern AP ice shelves (Figure 2a). Four of these jets (CI, MI, WI, MOI) have been studied using
198 airborne observations and model simulations (Grosvenor et al., 2014; Elvidge et al., 2016). The remaining three jets (LA,
199 LB, and JP) are, to our knowledge, identified here for the first time. Föhn winds form when moist air is forced over a
200 mountain barrier, often leading to precipitation on the windward side of the barrier that dries the air mass (Elvidge et al.,
201 2016). As the now drier air descends the leeward slope it warms adiabatically and promotes melt directly through sensible
202 heat exchange, and indirectly by the associated clear skies that allow additional shortwave radiation to reach the surface in
203 non-winter months (Elvidge et al., 2020; Laffin et al., 2021). Overall, winds from the west and northwest These positive
204 energy balance components increase surface melt rates up to 54% relative to non-föhn induced melt (Figure 2b).

205 ~~Additionally, AP winds from the west and northwest (föhn influence) produce surface melt rates twice as large as the~~
206 ~~average melt rate from all other wind directions (Figure 2c).~~ direction lead to increased surface melt rates that can be up to
207 53% higher than melt when the wind is from other directions (Figure 2c) (van den Broeke (2005)). Additionally, the degree
208 to which föhn winds impact surface melt on each ice shelf varies depending on föhn jet location and wind strength
209 (Wiesenekker et al., 2018). These variations may provide insight into why SCAR inlet and the LCIS remain intact while the
210 LAIS and LBIS have collapsed other than the significant difference in annual surface temperature (Cook and Vaughan
211 (2009); Bozkurt et al., 2020; Carrasco et al., 2021).

212



213

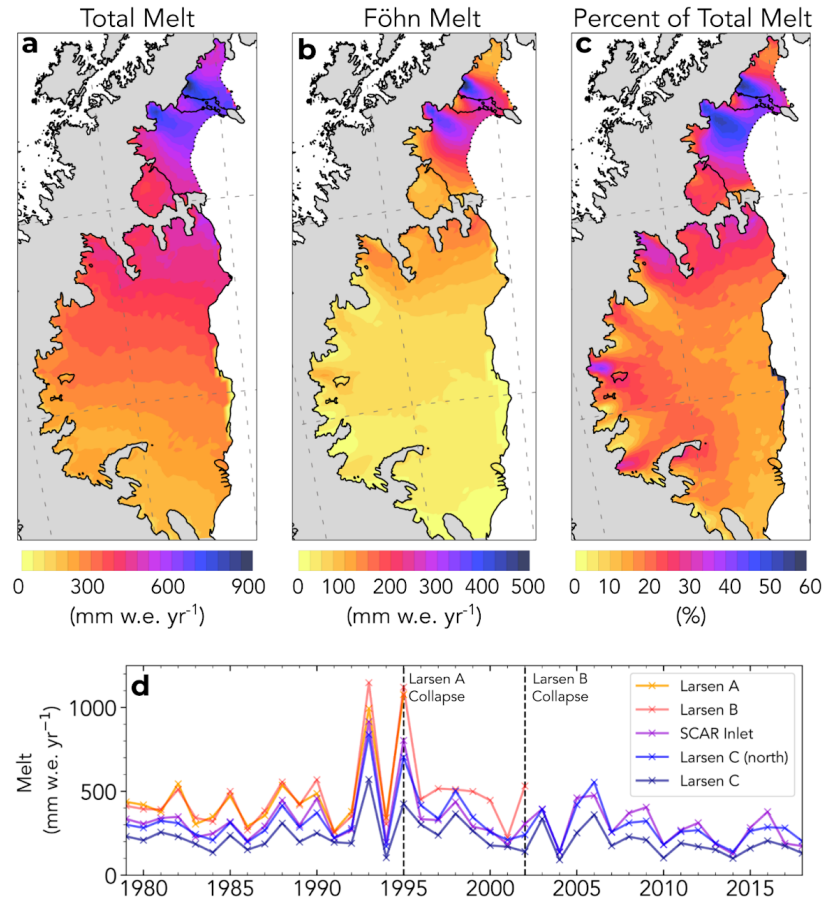


214 **Figure 2.** (a) The northern AP showing the RACMO2-simulated wind speed and direction vectors on January 24, 1995, just before the
 215 collapse of the LAIS. Föhn jet locations are indicated with names. (b) ▲ RACMO2 annual average föhn melt hour percent of total melt

216 hours and föhn melt percent of total melt surface melt hours and melt rate on each ice shelf during föhn (triangle) and non föhn (circle)
217 melt for each ice shelf from 1980-2002. (c) MRACMO2 melt rate as a function of wind direction averaged for all ice shelves shelf regions
218 on the AP from 1980-2002.

219
220 ~~The degree to which föhn winds impact surface melt on each ice shelf varies, and provides insight into why SCAR~~
221 ~~inlet and the LCIS remain intact while the LAIS and LBIS have collapsed other than the significant difference in annual~~
222 ~~surface temperature (Figure 5).~~ Surface melt production is more pronounced under the influence of föhn jets, particularly for
223 the LA and LB jets which produce 35.7% and 31.8% more melt respectively compared to regions not in the path of a föhn jet
224 on ~~the~~ each ice shelf shelf (Figure 3). Föhn-induced surface melt accounts for ~~32~~42% of the total annual melt between 1979
225 and 2002 on the LAIS and ~~47~~51% of total melt on the LBIS (~~Figure 3c~~) but only represents 21% and 25% of total melt hours
226 on the LAIS and LBIS (Figure 2b, 3c). In locations directly influenced by föhn jets, the mean annual föhn-induced melt was
227 as high as 61% on the LAIS and 57% on the LBIS of total annual melt. By contrast, föhn-induced melt accounts for only
228 ~~24~~5% of 1979-2002 total melt on SCAR inlet and 17% on the LCIS. SCAR inlet is not directly impacted by a föhn jet, but
229 still experiences clear skies and weak föhn influence ~~and clear skies from the overall descending air during föhn events~~. The
230 LCIS is affected by numerous föhn jets (CI, MI, WI, MOI), accounting for up to 40% of the total annual melt in Cabinet and
231 Whirlwind inlets, decreasing with distance east of the AP mountains. The stark contrast in surface melt amount and fraction
232 caused by föhn winds on collapsed vs. intact ice shelves implicates föhn melt as a contributor to the LAIS and LBIS
233 collapses. ~~However, no single factor, including föhn-induced melt rate, lessens the influence of all the other factors that~~
234 ~~contributed to these collapses~~. A clearer picture of the role of föhns emerges after we examine föhn-induced melt extent and
235 timing.

236 The spatial distribution and extent of surface melt influence ice shelf stability. Surface melt and melt lakes near the
237 ice shelf terminus can lead to calving front collapse and structural instability for the remaining portion of the ice shelf ~~vesf~~
238 (Depoorter et al., 2013; Pollard et al., 2015). Consistent with this mechanism, the LA and LB föhn jets impact a large spatial
239 area of the LAIS and LBIS, and reach the ice shelf calving fronts (Figure 3b). SCAR Inlet lacks a strong föhn jet/influence
240 and does not regularly experience largescale melt lakes even during high melt years (Figure 1b-f). This helps explain why
241 SCAR Inlet is still intact, despite major structural changes observed after the collapse of the LBIS (Borstad et al., 2016; Qiao
242 et al., 2020). LCIS on the other hand is impacted by four major jets and regularly experiences föhn-induced melt lakes,
243 particularly in Cabinet inlet. However, the vast size of the LCIS does not allow the föhn-induced melt to reach the terminus.
244 The föhn melt mechanism breaks down by mixing with cold air which reduces the intensity of the föhn jets from their peak
245 at the base of the AP mountains to the calving front (Figure 3b). Having established that föhn winds significantly enhanced
246 surface melt overall (Cape et al., 2015; Elvidge et al., 2015; Datta et al., 2019) and at the crucial calving front of LAIS and
247 LBIS, we now examine the timing of föhn-induced melt events relative to ~~the~~ collapses.



249 **Figure 3.** (a) **ARACMO2** average annual melt from 1980-2002. (b) **ARACMO2** average annual föhn wind-induced melt from 1980-2002.
 250 (c) **PRACMO2** percent of total melt concurrent with föhn wind from 1980-2002. (d) **FRACMO2** time series of the mean annual surface
 251 melt on each ice shelf from 1979-2018. Dashed vertical lines indicate the year in which each ice shelf collapsed. Note: The Larsen B curve
 252 often overlaps the Larsen A curve.

253 3.2 Coincidence of föhn winds with collapse

254 3.2.1 LAIS

255 Three föhn wind events occurred on LAIS between January 18 and 27, 1995, overlapping with the initial phase of the LAIS
 256 collapse that began on January 25 (Figure 4b) (Rott et al., 1998). These föhn events helped contribute to the collapse of
 257 the ice shelf in two ways: (1) The west/northwest wind direction actively pushed or melted sea ice and fast ice away from the
 258 calving front, allowing ocean waves to reach the terminus (Massom et al., 2018); (2) Enhanced surface melt rates caused by
 259 the LA jet led to extensive melt lakes across the ice shelf that promoted large scale hydrofracture cascades when the ice shelf
 260 terminus was breached (Banwell et al., 2013). These föhn wind events prior to and during collapse lasted an average of 3

261 days each and produced increased surface melt greater than any other 9-day period from 1979-2018, with mean cumulative
262 melt of 268.5 mm w.e. or 25.2% of the total annual melt in the 1994/95 melt season. Total melt during the 1994/95 melt
263 season was 127% higher than an average year (474 mm w.e./yr) and the 9-day föhn wind event produced 57% of the total
264 melt of an average melt year. Therefore this 9-day föhn-induced melt event and melt year are clearly anomalous in the
265 observational record.

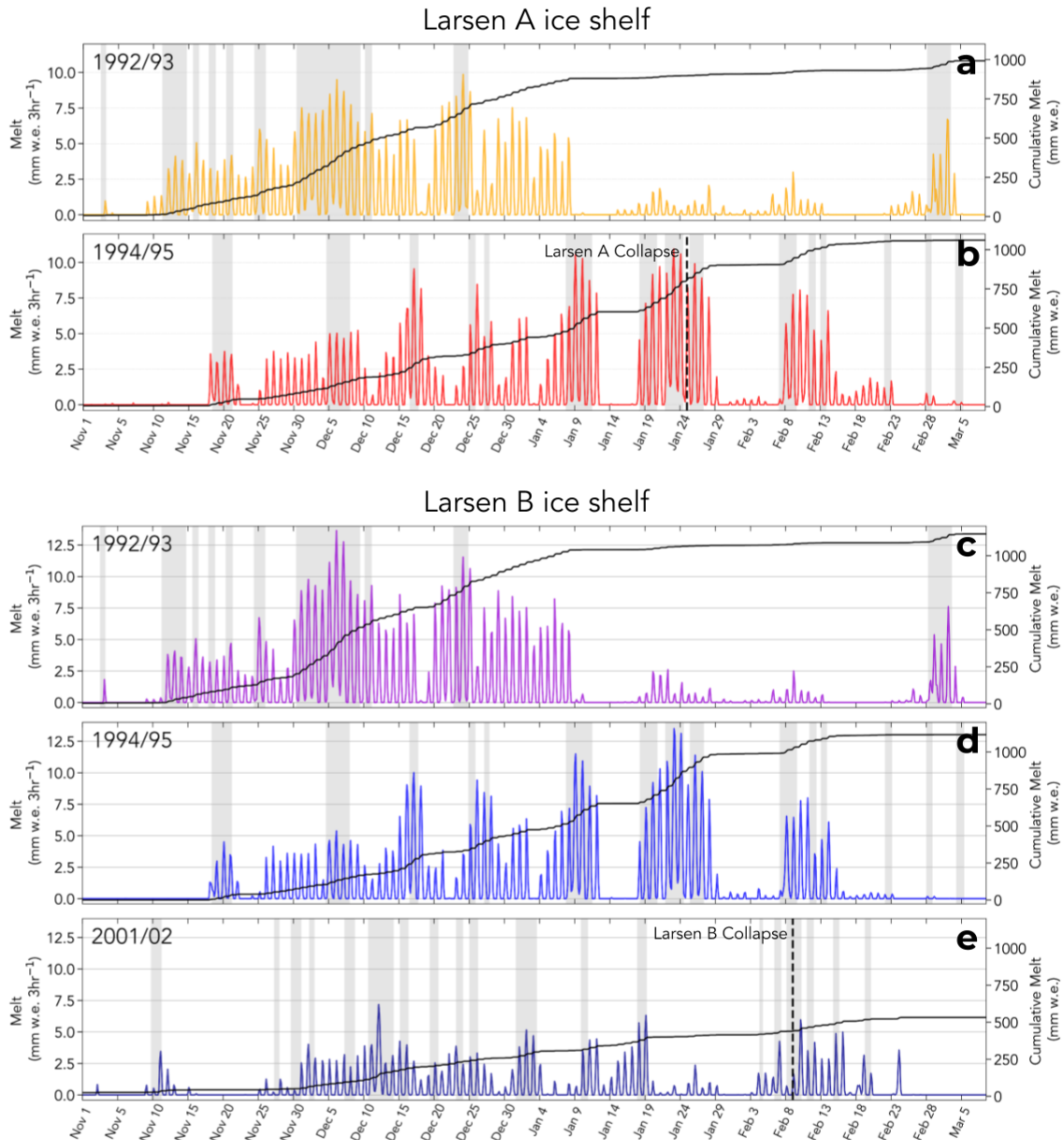
266 We next examine the contribution of föhn-generated melt to other observables implicated in the collapse, namely
267 surface liquid water, melt lake depth, and melt lake extent (Scambos et al., 2003; ~~Banwell et al., 2013~~). We estimate the
268 spatial extent and depth of melt lakes prior to collapse on the LAIS using satellite images of melt lake surface area combined
269 with model-simulated available liquid water volume. The cumulative spatial melt pattern between January 18 and 27, 1995
270 identifies significant melt on the LAIS ranging from 157-356 mm w.e. (Figure S+2a), varying spatially with the influence of
271 the LA jet. Satellite imagery of the LAIS during ~~the collapse does not yield high enough resolution to decipher melt in~~
272 ~~progress show melt lakes were present (Figure S3) however because the collapse had already begun, it is likely many of the~~
273 ~~lakes had drained or had been altered lake surface area so estimating melt lake extent is not possible.~~ However, Advanced
274 Very High-Resolution Radiometer (AVHRR) imagery on December 8, 1992, provides high-resolution cloudless images of
275 the ice shelf taken at the end of a similar föhn-induced melt event during a year when melt was comparable to the 1994/95
276 melt season, therefore we consider this melt lake extent analogous to the 1994/95 melt season (Figure 4a). We find the melt
277 lake surface area was likely between 5.1%-10.8% (103 km² - 219 km²) of the total LAIS surface area (Figure S+2b). Melt
278 lake surface area is likely underestimated because the image was taken early in the 1992/93 melt season and does not easily
279 identify small lakes or river systems. Liquid water pooling on the ice surface is modulated by the local topography. If we
280 assume all the available surface liquid water during the 9-day melt period, minus evaporation, runoff, and refreeze, forms
281 lakes that cover the same estimated surface area as the 1992/93 melt season, we can estimate melt lake depth during the
282 initial collapse. We find mean melt lake depth to be between 1.38-6.86 meters depending on lake location and föhn
283 influence, which exceeds the average lake depth of the LBIS lakes prior to collapse (1 meter) and the critical lake depth that
284 was identified in LBIS collapse ~~modeling/modelling~~ studies (3.5 m), especially under the influence of the LA jet (Banwell et
285 al., 2013).

286

287 3.2.2 LBIS

288 A föhn wind event coincided with the initial LBIS collapse on February 9, 2002, with ~~two events just prior to collapse and~~
289 ~~three additional events before~~ complete collapse by March 17, 2002 (Figure 4c). ~~In contrast to föhn pre-cursors of the LAIS~~
290 ~~collapse,~~ föhn events in the LBIS 2001/02 melt season were relatively short, averaging less than 24 hours per event, and
291 produced melt rates ~~just~~ 27% higher than non-föhn melt that year and ~~only~~ 39% of the average föhn melt rate in all other
292 years (Figure 4e). ~~Similar to the LAIS collapse the off-coast wind direction and enhanced surface melt rates during the föhn~~

293 wind event helped push sea ice away from the calving front and contributed to surface melt lakes that led to hydrofracture
 294 and collapse. We conclude that while enhanced surface melt from föhn winds likely triggered the LAIS collapse, the LBIS
 295 collapse was not directly related to the impact of föhn-induced melt. Nevertheless, previous high melt rate
 296 föhn events such as those in the 1992/93 and 1994/95 melt seasons likely preconditioned the LBIS through firm densification
 297 to support melt lake formation, discussed in section 3.3.



298

299 **Figure 4.** RACMO2 time series of surface melt production and cumulative melt during the Antarctic melt season averaged over the
300 indicated ice shelf. Grey shading indicates the presence of föhn winds. (a) 1992/1993 LAIS. (b) 1994/1995 LAIS. (c) 1992/1993 LBIS. (d)
301 1994/1995 LBIS. (e) 2001/2002 LBIS. *Note:* Surface melt that occurs after the collapse events indicated by the dashed vertical lines in (b)
302 and (e) are estimates of melt quantity if the ice shelves did not disintegrate.

303 3.3 Föhn melt and the surface liquid water budget

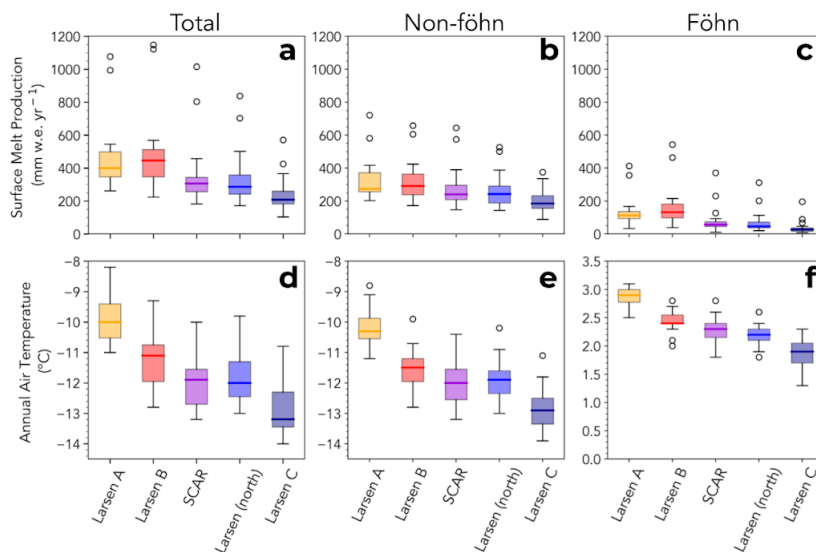
304 To better understand the role that föhn winds have played in AP ice shelf surface melt and stability we intercompare melt
305 climatologies and the surface liquid water budget of all major ice shelves. Comparing a comparison of collapsed with intact
306 ice shelves yields a clearer picture of the effects föhn winds have on ice shelf stability. We identify whether annual surface
307 melt production, melt rate, melt hours, and surface temperature variables from 1980-2002 are significantly different from the
308 LBIS (Figure 5 and corresponding two-tailed t-test statistics in Table S+2). We compare to LBIS because it was
309 centered between other ice shelves and was the most recent to collapse. Total surface melt production on every ice
310 shelf except LAIS differs significantly from LBIS melt (Mean annual melt over the ice shelf area; LAIS-476 mm w.e.,
311 LBIS-479 mm w.e., SCAR-353 mm w.e., Larsen(north)-336 mm w.e., LCIS-238 mm w.e.) (Figure 5a), which is expected
312 when we consider the latitudinal location and mean annual air temperature (Figure 5d) (Table S+2). However, when
313 föhn-induced melt is subtracted from total melt, the mean annual surface melt production on SCAR inlet and Larsen C
314 (north) are not statistically different from the LBIS (LAIS-337 mm w.e., LBIS-321 mm w.e., SCAR-286 mm w.e.,
315 Larsen(north)-278 mm w.e., LCIS-203 mm w.e.) (Figure 5b). In other words, with the exception of föhn-induced melt
316 (Figure 5c), melt production on SCAR Inlet and LCIS are statistically indistinguishable at the 95% confidence interval from
317 LBIS melt production. Föhn wind-induced surface melt impacted the collapsed ice shelves significantly more than extant ice
318 shelves which further implicates defines föhn melt as an important contributor to LAIS and possibly LBIS melt budget
319 collapse. The relatively small role that föhns play in the liquid water production and variability on the remaining ice shelves
320 bodes well for their continued resilience.

321 The nominal amount of föhn-induced melt on the LBIS in the 2001/02 melt season nevertheless played a role in ice
322 shelf stability through firm densification. Our analysis of firm density or available firm pore space identifies significant
323 differences in ice shelves that have collapsed and those that remain intact. Firm densification occurs when the liquid water
324 fills the pore space between snow/ice crystals decreasing the air content in the firm, which forms refrozen ice layers that
325 promote melt lake formation (Kuipers Munneke et al., 2012; Polashenski et al., 2017). A liquid-to-solid ratio (LSR) is a
326 crude proxy for available firm air content and can be estimated as;

$$328 \quad LSR = \frac{\text{Total liquid water (snowmelt + liquid precipitation)}}{\text{Total solid precipitation (snow)}} \quad (1)$$

329

330 where areas with $LSR < 1$ represent an ice shelf that receives more solid precipitation than liquid water and is therefore less
 331 likely to saturate with liquid water and form melt lakes than areas with $LSR > 1$ (Figure 6). The liquid-to-solid ratio (LSR) is
 332 a crude proxy for available firm air content. Extant ice shelves (SCAR inlet, LCIS) have an LSR just above 1 for the
 333 period 1980-2002 if all surface melt is included (Figure 6a). The LSR for LAIS and LBIS is also just above 1 for this period,
 334 though only if föhn-induced surface melt is excluded. However, when surface melt caused by föhn wind is included, LSR
 335 exceeds 1.5 throughout extensive regions, including the ice shelf margins, of the LAIS and LBIS. Thus the collapsed ice
 336 shelves experienced climatological LSRs significantly larger than the extant ice shelves, mainly due to föhn-induced melt.
 337 This ~~again~~ result suggests that föhn-induced melt helped precondition the LAIS and LBIS to ~~collapse~~ produce extensive melt
 338 lakes by long-term firm densification.

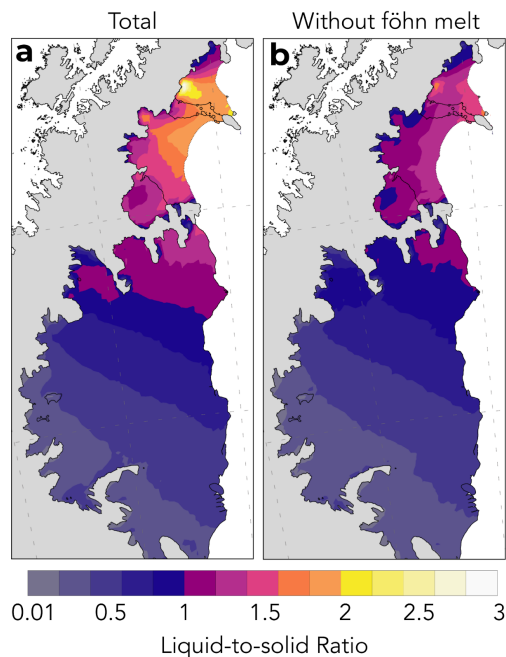


339

340 **Figure 5.** Box and whisker plots intercompare ice shelves with RACMO2 data-simulations from 1980-2002. **A** Annual surface melt
 341 production (a) all melt, (b) non-föhn melt, (c) föhn-induced melt. (d) Mean annual air temperature, (e) air temperature without föhn winds,
 342 (f) air temperature during föhn winds. *Note:* the LAIS estimates are hypothetical after 1995, but are still resolved in the model simulations.

343

344



345

346 **Figure 6.** FRACMO2 firn liquid-to-solid ratio or mean annual liquid water divided by mean annual frozen precipitation for (a) total melt
 347 and (b) all liquid water except föhn-induced melt. *Note:* the LAIS estimates are hypothetical after 1995, but are still resolved in the model
 348 simulations.

349 4 Discussion

350 ~~It is reasonable to expect differences in ice shelf melt regime, particularly with~~ The north/south temperature gradient present
 351 on the eastern AP ice shelves contributes to the differences in the ice shelf melt regime (Figure 5). ~~The annual surface~~
 352 ~~temperature difference between ice shelves could explain ice shelf disintegration through long-term thinning and~~
 353 ~~retreat~~ Warmer ice shelves can be more vulnerable to long-term thinning and retreat that accelerate disintegration (Scambos
 354 et al., 2003; Morris ~~et al.~~ and Vaughan (2003)). ~~However, the~~ temperature gradient alone ~~cannot~~ does not explain the
 355 substantial increase in surface melt on the LAIS and LBIS ~~relative to more southerly ice shelves~~. Only with the addition of
 356 föhn-induced ~~surface melt~~ (Figure 5c) do the LAIS and LBIS stand out significantly from the other eastern AP ice shelves
 357 (Figure 5a,b). With that in mind, we have examined liquid water processes on the spatio-temporal scales pertinent to AP ice
 358 shelf stability. For instance, the structural flow discontinuities or suture zones, where tributary glaciers merge together to
 359 form an ice shelf, are mechanically weak points that impact stability (Glasser ~~et al., 2008~~ Sandhager et al., 2005; Glasser and
 360 Scambos (2008); Glasser et al., 2009). These suture zones are further weakened through lateral shear depending on the
 361 difference in tributary glacier flow. All ice shelves in the region are ~~comprised~~ composed of numerous outflow glaciers
 362 sutured together, and while some studies suggest this is a major contributor to ice shelf instability, only two of the ice shelves

363 have collapsed (Borstad et al., 2016; Glasser ~~et al.~~ and Scambos (2008); ~~Glasser et al. 2021~~). Further research suggests that
364 marine accretion of ice on the bottom of the ice shelves, specifically LCIS, may ~~stabilize~~ stabilise these suture zones, which
365 may be why SCAR inlet has remained intact despite major rift formation (McGrath et al., 2014; Borstad et al., 2016).

366 The timing of surface melt and melt enhanced by föhn winds within the melt season may also provides insight into
367 the fate of LAIS and LBIS, including why neither ice shelf collapsed in the anomalously strong 1992/93 melt season (Figure
368 3d). Pore space within the upper snow and firn layers buffers surface melt before lakes begin to form (Polashenski et al.,
369 2017). Late season melt is more likely to form surface melt lakes because meltwater from the preceding fall, winter, and
370 spring has partially or completely filled available pore space. On both the LAIS and LBIS, 92% of surface melt during the
371 1992/93 melt season occurred before January 9th when there was more pore space to buffer the anomalous surface melt than
372 at the onsets of their collapses in late January 1995 and early February 2002, respectively (Figure 4a, c). Melt lakes were
373 present on both ice shelves throughout the 1992/93 melt season, though melt production slowed dramatically after
374 mid-January, 1993 (Scambos et al., 2000). The high melt rates in late November and early December 1992 on the LAIS were
375 perhaps too early in the melt season, and after too many years of nominal melt, to form substantial melt lakes and trigger
376 hydrofracture that season. Nevertheless, the 1992/93 melt could have preconditioned the shelf for collapse in January 1995.
377 The LBIS collapse began in February 2002 after the surface melt had returned to nominal, 1980s levels for six years. How
378 much pore space had recovered during those six years is unknown, and an important question for future research. Satellite
379 images of surface melt lakes indicate 11% of the ice shelf was covered in melt lakes prior to collapse (Glasser ~~et al.~~ and
380 Scambos (2008)). However, the preceding melt year (2000/2001) had low melt and high precipitation, which added
381 additional snow mass to the unstable ice shelf (Leeson et al., 2017).

382 Another possible reason collapse did not occur in the 92/93 melt season or other years prior to collapse was a
383 possible misalignment of the four prerequisites for rapid collapse theorised by Massom et al., (2018). An AVHRR image of
384 the LAIS taken on December 8, 1992, just after a series of major föhn wind events that lead to 252 mm w.e. of surface melt
385 in the 8 days prior to the image (Figure 4a), show significant melt lakes across the LAIS, which make hydrofracture cascades
386 possible. However, in the same image, sea ice/melange are shown to be at the calving front, protecting the front from large
387 ocean waves that could trigger collapse. It may have been too early in the melt season to have substantial gaps in sea ice, the
388 ocean temperature may have been too cold, ocean circulation could have help stabilise the sea ice at the front, the föhn winds
389 speed could have been too weak to push the ice away or may have been in the wrong direction, all of which could have not
390 allowed a proper trigger for collapse even though substantial melt ponds were present. Even if there were years or instances
391 that sea ice extent was low and substantial melt lakes were present, there could have been a lack of large period ocean swells
392 that are thought to trigger collapse.

393 Regardless of other possible contributors to ice shelf instability not considered here (e.g., basal warming),
394 föhn-induced surface melt and associated melt lakes, and the off-coast wind direction likely ~~were a likely~~ played an important

395 role ~~trigger that in pushed~~ pushing the LAIS and LBIS past a structural tipping point. The estimated surface melt lake depth
396 caused by the 9-day föhn melt event on the LAIS surpassed the critical melt lake depth of stability identified by model
397 studies and satellite-derived ~~of the LBIS collapse and satellite-derived~~ lake depths before the collapse of the LBIS (Banwell
398 et al., 2013). The LAIS was likely the same thickness (200m) or thinner at the time of collapse so the estimate of critical
399 surface lake depth for the LBIS that is applied to the LAIS may reflect an upper limit of melt lake depth of stability for the
400 LAIS. Melt lake depth is likely underestimated because our estimation only accounts for melt during the 9-day melt event.
401 Melt before this time period already exceeded an average melt year by 23% (118 mm w.e.) so melt lakes probably already
402 existed. ~~The large melt volume in a relatively short amount of time spatially expanded and increased melt lake formation and~~
403 ~~depth, filled crevasses, increased water pressure on the crevasse tip and walls and triggered large-scale hydrofracture~~
404 ~~cascades that led to catastrophic disintegration of the LAIS (Scambos et al., 2000; Banwell et al., 2013). The same cannot be~~
405 ~~said about the LBIS. Föhn-driven melt alone cannot convincingly explain the LBIS collapse in 2002 because föhn melt was~~
406 ~~even stronger in at least two prior seasons, 1992-93 and 1994-95. It is more likely that a combination of changes to LBIS~~
407 ~~structure (flow speed, suture zones, thinning), ocean forcing (ocean warming, sea ice loss, and wave action), and~~
408 ~~atmospheric forcing (precipitation, temperature, föhn winds), pushed it across a natural threshold of environmental factors~~
409 ~~and ultimately led LBIS to collapse.~~

410 5 Conclusions

411 The converging lines of evidence in these results show, ~~for the first time,~~ that observed and inferred föhn-driven melt is
412 present in sufficient amounts, and at the right locations and times, to cause extensive surface melt lakes, while the off-coast
413 föhn wind direction pushed sea ice away from the calving front. ~~explain the disintegration of Larsen A in 1995 but not~~
414 ~~Larsen B in 2002.~~ The fact that the LAIS and LBIS collapsed catastrophically within weeks and not through long-term
415 thinning and retreat like other ice shelves (Prince Gustav, Wordie, ~~George VI~~) suggests sudden disintegration is anomalous
416 and requires forcings to match vulnerabilities (Scambos et al., 2003). We conclude that föhn winds and the
417 ~~associated-induced~~ surface melt ~~was a trigger for~~ played a significant role in the collapses of the LAIS ~~but not the~~ and LBIS-
418 ~~The~~, while remaining extant AP ice shelves ~~may be more stable, at least from melt-driven instability, than previously~~
419 ~~thought~~ are not likely to collapse from föhn-induced melt and hydrofracture in today's current climate. We have come to these
420 conclusions with the following forms of evidence:

421

- 422 • First, both the LAIS and LBIS are impacted by powerful melt-inducing föhn jets that affect a large spatial portion of
423 each ice shelf ~~that and~~ reach the ice shelf terminus. Surface melt and melt lakes near the ice shelf terminus can lead
424 to calving front collapse and structural instability for the remaining portion of the ice shelves (Depoorter et al.,

425 2013; Pollard et al., 2015; ~~Depoorter et al., 2013~~). Extant ice shelves are either not directly affected by a föhn jet, ~~or~~
426 are too vast to have any significant effect near the terminus, ~~or are too far south to experience major melt events.~~

- 427 • Second, strong föhn winds were present prior to and ~~at the time of~~during collapse for the LAIS and LBIS. ~~This~~A
428 series of ~~three~~ föhn events on the LAIS lasted nine days total and produced over 25% of the total annual melt for
429 the 1994/95 melt season, while föhn was present prior to and during the collapse of the LBIS which enhanced
430 surface melt rates. ~~The~~Enhanced melt, filled new and existing melt ~~ponds~~lakes above the critical (1 meter) melt
431 lake depth of stability ~~which ultimately triggered large-scale hydrofracture cascades and the LAIS collapse. A föhn~~
432 ~~event was also present at the onset of the LBIS collapse, however, melt rates were nominal and likely did not~~
433 ~~produce a trigger effect.~~ The föhn winds on both ice shelves actively pushed sea ice away from the calving front
434 allowing large period ocean swells to trigger large scale hydrofracture cascades exacerbated by extensive surface
435 melt and originated from the ice shelf terminus.
- 436 • Third, in the absence of föhn wind ~~and concurrent~~-induced melt, the surface liquid budgets of collapsed and intact
437 ice shelves are climatically similar, which points to föhn winds as a driver of increased surface melt and ~~possibly~~
438 ~~rapid collapse~~extensive melt lakes on collapsed ice shelves. The additional föhn induced ~~-~~melt on the LAIS and
439 LBIS compared to intact ice shelves ~~created impermeable ice layers that support melt lake production, particularly~~
440 ~~when annual surface melt exceeds annual precipitation~~helped precondition the LAIS and LBIS to produce extensive
441 melt lakes by long-term firn densification.

442

443 ~~We acknowledge the subjectivity of labeling any of the causal factors that led to the LAIS or LBIS ice shelf~~
444 ~~collapses as a trigger when many factors contributed to the collapses. Nevertheless, †~~This research clarifies the roles of
445 föhn-induced melt for collapsed and extant ice shelves. Future ~~forensic~~ analyses of these ice shelf collapse events using
446 advanced firn density models coupled with ice-ocean-atmospheric coupled simulations may be useful to better understand
447 the role of surface melt in ice shelf instability. Further, the AP föhn wind regime has remained stable over the past
448 half-century (Laffin et al., 2021) which points to enhanced surface temperatures and increased liquid phase precipitation as
449 more important contributors to the future surface liquid budget on remaining ice shelves and is an important area of future
450 research (Bozkurt et al., 2020; Bozkurt et al., 2021). However, changes in climate drivers such as the Southern Annular
451 Mode (SAM), which influences the north-south movement of the westerlies in the region, may alter the temperature and föhn
452 occurrence that will likely enhance surface melt in locations farther south, and therefore make morth southern ice shelves
453 more vulnerable (Abram et al., 2014; Zheng et al., 2013; Lim et al., 2016;). Nevertheless, ~~†~~ this research highlights a new
454 understanding behind surface melt mechanisms for ice shelf collapse and suggests that extant ice shelves in the region may
455 remain stable so long as surface liquid water from melt and precipitation remains within historical bounds.

456

457

458 *Author contributions.* M.K.L and C.S.Z designed the study. M.V.W. and S.M. curated the model simulation output and
459 surface observations. M.K.L performed statistical data analysis. M.K.L. wrote the article with valuable input from all
460 authors.

461

462 *Competing interests.* The authors declare no conflict of interest.

463

464 *Acknowledgments.* MKL was supported by the National Science Foundation (NRT-1633631) and NASA AIST
465 (80NSSC17K0540). CSZ gratefully acknowledges support from the DOE BER ESM and SciDAC programs
466 (DE-SC0019278, LLNL-B639667, LANL-520117). JMWV acknowledges support by PROTECT and was partly funded by
467 the NWO (Netherlands Organisation for Scientific Research) VENI grant VI.Veni.192.083. [We thank Dr. Helmut Rott for](#)
468 [generously providing detailed in-person observations of the LAIS months before collapse.](#) We also thank the Institute for
469 Marine and Atmospheric research Utrecht (IMAU) for providing RACMO2 output. RACMO2 model data are available by
470 request at <https://www.projects.science.uu.nl/iceclimate/models/antarctica.php>, however, a subset (2001-2018) of the data are
471 hosted online at <https://zenodo.org/record/3677642#.X-pXAFNKjUI>.

472 **References**

- 473 ~~Adusumilli, S., Fricker, H. A., Siegfried, M. R., Padman, L., Paolo, F. S. and Ligtenberg, S. R. M.: Variable Basal Melt Rates~~
474 ~~of Antarctic Peninsula Ice Shelves, 1994–2016, *Geophys. Res. Lett.*, 45(9), 4086–4095, doi:10.1002/2017GL076652,~~
475 ~~2018.~~
- 476 ~~Alley, K. E., Scambos, T. A., Miller, J. Z., Long, D. G. and MacFerrin, M.: Quantifying vulnerability of Antarctic ice shelves~~
477 ~~to hydrofracture using microwave scattering properties, *Remote Sens. Environ.*, 210, 297–306,~~
478 ~~doi:10.1016/j.rse.2018.03.025, 2018.~~
- 479 ~~Banwell, A. F., MacAyeal, D. R. and Sergienko, O. V.: Breakup of the Larsen B Ice Shelf triggered by chain reaction~~
480 ~~drainage of supraglacial lakes, *Geophys. Res. Lett.*, 40(22), 5872–5876, doi:10.1002/2013GL057694, 2013.~~
- 481 ~~Banwell, A. F., Willis, I. C., Macdonald, G. J., Goodsell, B. and MacAyeal, D. R.: Direct measurements of ice-shelf flexure~~
482 ~~caused by surface meltwater ponding and drainage, *Nat. Commun.*, 10(1), doi:10.1038/s41467-019-08522-5, 2019.~~
- 483 ~~Bell, R. E., Banwell, A. F., Trusel, L. D. and Kingslake, J.: Antarctic surface hydrology and impacts on ice-sheet mass~~
484 ~~balance, *Nat. Clim. Chang.*, 8(12), 1044–1052, doi:10.1038/s41558-018-0326-3, 2018.~~
- 485 ~~Borstad, C., Khazendar, A., Scheuchl, B., Morlighem, M., Larour, E. and Rignot, E.: A constitutive framework for predicting~~
486 ~~weakening and reduced buttressing of ice shelves based on observations of the progressive deterioration of the remnant~~
487 ~~Larsen B Ice Shelf, *Geophys. Res. Lett.*, 43(5), 2027–2035, doi:10.1002/2015GL067365, 2016.~~

488 ~~Bozkurt, D., Bromwich, D. H., Carraseo, J., Hines, K. M., Maureira, J. C. and Rondanelli, R.: Recent Near-surface~~
489 ~~Temperature Trends in the Antarctic Peninsula from Observed, Reanalysis and Regional Climate Model Data, Adv.~~
490 ~~Atmos. Sci., 37(5), 477–493, doi:10.1007/s00376-020-9183-x, 2020.~~

491 ~~Bozkurt, D., Bromwich, D. H., Carraseo, J. and Rondanelli, R.: Temperature and precipitation projections for the Antarctic~~
492 ~~Peninsula over the next two decades: contrasting global and regional climate model simulations, Clim. Dyn.,~~
493 ~~doi:10.1007/s00382-021-05667-2, 2021.~~

494 ~~Braun, M. and Humbert, A.: Recent retreat of wilkins ice shelf reveals new insights in ice shelf breakup mechanisms, IEEE~~
495 ~~Geosci. Remote Sens. Lett., 6(2), 263–267, doi:10.1109/LGRS.2008.2011925, 2009.~~

496 ~~Depoorter, M. A., Bamber, J. L., Griggs, J. A., Lenaerts, J. T. M., Ligtenberg, S. R. M., Van Den Broeke, M. R. and Moholdt,~~
497 ~~G.: Calving fluxes and basal melt rates of Antarctic ice shelves, Nature, 502(7469), 89–92, doi:10.1038/nature12567,~~
498 ~~2013.~~

499 ~~Elvidge, A. D., Kuipers Munneke, P., King, J. C., Renfrew, I. A. and Gilbert, E.: Atmospheric Drivers of Melt on Larsen C~~
500 ~~Ice Shelf: Surface Energy Budget Regimes and the Impact of Foehn, J. Geophys. Res. Atmos., 125(17),~~
501 ~~doi:10.1029/2020JD032463, 2020.~~

502 ~~Elvidge, A. D., Renfrew, I. A., King, J. C., Orr, A., Lachlan-Cope, T. A., Weeks, M. and Gray, S. L.: Foehn jets over the~~
503 ~~Larsen C Ice Shelf, Antarctica, Q. J. R. Meteorol. Soc., 141(688), 698–713, doi:10.1002/qj.2382, 2015.~~

504 ~~Glasser, N. F. and Scambos, T. A.: A structural glaciological analysis of the 2002 Larsen B ice-shelf collapse, J. Glaciol.,~~
505 ~~54(184), 3–16, doi:10.3189/002214308784409017, 2008.~~

506 ~~Glasser, N. F., Kulesa, B., Luckman, A., Jansen, D., King, E. C., Sammonds, P. R., Scambos, T. A. and Jezek, K. C.:~~
507 ~~Surface structure and stability of the Larsen C ice shelf, Antarctic Peninsula, 2009.~~

508 ~~Gudmundsson, G. H.: Ice-shelf buttressing and the stability of marine ice sheets, Cryosphere, 7(2), 647–655,~~
509 ~~doi:10.5194/te-7-647-2013, 2013.~~

510 ~~Kuipers Munneke, P., Van Den Broeke, M. R., King, J. C., Gray, T. and Reijmer, C. H.: Near-surface climate and surface~~
511 ~~energy budget of Larsen C ice shelf, Antarctic Peninsula, Cryosphere, 6(2), 353–363, doi:10.5194/te-6-353-2012, 2012.~~

512 ~~Laffin, M. K., Zender, C. S., Singh, S., Van Wessem, J. M., Smeets, C. J. P. P. and Reijmer, C. H.: Climatology and~~
513 ~~Evolution of the Antarctic Peninsula Föhn Wind-Induced Melt Regime From 1979–2018, J. Geophys. Res. Atmos.,~~
514 ~~126(4), doi:10.1029/2020JD033682, 2021.~~

515 ~~Leeson, A. A., Van Wessem, J. M., Ligtenberg, S. R. M., Shepherd, A., Van Den Broeke, M. R., Killick, R., Skvarca, P.,~~
516 ~~Marinsck, S. and Colwell, S.: Regional climate of the Larsen B embayment 1980–2014, J. Glaciol., 63(240), 683–690,~~
517 ~~doi:10.1017/jog.2017.39, 2017.~~

518 ~~Mahaffy, P. R., Webster, C. R., Atreya, S. K., Franz, H., Wong, M., Conrad, P. G., Harpold, D., Jones, J. J., Leshin, L. A.,~~
519 ~~Manning, H., Owen, T., Pepin, R. O., Squyres, S. and Trainer, M.: Abundance and isotopic composition of gases in the~~

520 ~~martian atmosphere from the Curiosity rover, *Science* (80), 341(6143), 263–266, doi:10.1126/science.1237966, 2013.~~

521 ~~Massom, R. A., Scambos, T. A., Bennetts, L. G., Reid, P., Squire, V. A. and Stammerjohn, S. E.: Antarctic ice shelf~~

522 ~~disintegration triggered by sea ice loss and ocean swell, *Nature*, 558(7710), 383–389, doi:10.1038/s41586-018-0212-1,~~

523 ~~2018.~~

524 ~~Mattia Poinelli, I., Schodlok, M. and Larour, E.: Modeling of Ocean Dynamics in Ice-Shelf Rifts, *ESSOAr*,~~

525 ~~doi:10.1002/essoar.10506246.2, 2021.~~

526 ~~McGrath, D., Steffen, K., Holland, P. R., Scambos, T., Rajaram, H., Abdalati, W. and Rignot, E.: The structure and effect of~~

527 ~~suture zones in the Larsen C Ice Shelf, *Antarctica, J. Geophys. Res. Earth Surf.*, 119(3), 588–602,~~

528 ~~doi:10.1002/2013JF002935, 2014.~~

529 ~~Mulvaney, R., Abram, N. J., Hindmarsh, R. C. A., Arrowsmith, C., Fleet, L., Triest, J., Sime, L. C., Alemany, O. and Foord,~~

530 ~~S.: Recent Antarctic Peninsula warming relative to Holocene climate and ice-shelf history, *Nature*, 489(7414), 141–144,~~

531 ~~doi:10.1038/nature11391, 2012.~~

532 ~~Polashenski, C., Golden, K. M., Perovich, D. K., Skyllingstad, E., Arnsten, A., Stwertka, C. and Wright, N.: Percolation~~

533 ~~blockage: A process that enables melt pond formation on first year Arctic sea ice, *J. Geophys. Res. Ocean.*, 122(1),~~

534 ~~413–440, doi:10.1002/2016JC011994, 2017.~~

535 ~~Pollard, D., DeConto, R. M. and Alley, R. B.: Potential Antarctic Ice Sheet retreat driven by hydrofracturing and ice cliff~~

536 ~~failure, *Earth Planet. Sci. Lett.*, 412, 112–121, doi:10.1016/j.epsl.2014.12.035, 2015.~~

537 ~~Pritchard, H. D., Ligtenberg, S. R. M., Fricker, H. A., Vaughan, D. G., Van Den Broeke, M. R. and Padman, L.: Antarctic~~

538 ~~ice-sheet loss driven by basal melting of ice shelves, *Nature*, 484(7395), 502–505, doi:10.1038/nature10968, 2012.~~

539 ~~Qiao, G., Li, Y., Guo, S. and Ye, W.: Evolving instability of the scar inlet ice shelf based on sequential landsat images~~

540 ~~spanning 2005–2018, *Remote Sens.*, 12(1), doi:10.3390/RS12010036, 2020.~~

541 ~~Rignot, E., Casassa, G., Gogineni, P., Krabill, W., Rivera, A. and Thomas, R.: Accelerated ice discharge from the Antarctic~~

542 ~~Peninsula following the collapse of Larsen B ice shelf, *Geophys. Res. Lett.*, 31(18), doi:10.1029/2004GL020697, 2004.~~

543 ~~Robel, A. A. and Banwell, A. F.: A Speed Limit on Ice Shelf Collapse Through Hydrofracture, *Geophys. Res. Lett.*, 46(21),~~

544 ~~12092–12100, doi:10.1029/2019GL084397, 2019.~~

545 ~~Rott, H., Rack, W., Nagler, T. and Skvarca, P.: Climatically induced retreat and collapse of norther Larsen Ice Shelf;~~

546 ~~Antarctic Peninsula, *Ann. Glaciol.*, 27, 86–92, doi:10.3189/s0260305500017262, 1998.~~

547 ~~Sandhäger, H., Rack, W. and Jansen, D.: Model investigations of Larsen B Ice Shelf dynamics prior to the breakup. [online]~~

548 ~~Available from: <http://www.uib.no/People/ngfls/frisp/Rep16/sandhageretal.pdf>, 2005.~~

549 ~~Scambos, T. A., Hulbe, C., Fahnestock, M. and Bohlander, J.: The link between climate warming and break-up of ice shelves~~

550 ~~in the Antarctic Peninsula, *J. Glaciol.*, 46(154), 516–530, doi:10.3189/172756500781833043, 2000.~~

551 ~~Scambos, T., Hulbe, C. and Fahnestock, M.: Climate-Induced Ice Shelf Disintegration in the Antarctic Peninsula, pp. 79–92.,~~

552 ~~2013.~~

553 ~~Schodlok, M. P., Menemenlis, D. and Rignot, E. J.: Ice shelf basal melt rates around Antarctica from simulations and~~
554 ~~observations, J. Geophys. Res. Ocean., 121(2), 1085–1109, doi:10.1002/2015JC011117, 2016.~~

555 ~~Trusel, L. D., Frey, K. E., Das, S. B., Karnauskas, K. B., Kuipers Munneke, P., Van Meijgaard, E. and Van Den Broeke, M.~~
556 ~~R.: Divergent trajectories of Antarctic surface melt under two twenty-first-century climate scenarios, Nat. Geosci.,~~
557 ~~8(12), 927–932, doi:10.1038/ngeo2563, 2015.~~

558 ~~Trusel, L. D., Frey, K. E., Das, S. B., Munneke, P. K. and Van Den Broeke, M. R.: Satellite-based estimates of Antarctic~~
559 ~~surface meltwater fluxes, Geophys. Res. Lett., 40(23), 6148–6153, doi:10.1002/2013GL058138, 2013.~~

560 ~~Van den Broeke, M.: Strong surface melting preceded collapse of Antarctic Peninsula ice shelf, Geophys. Res. Lett., 32(12),~~
561 ~~1–4, doi:10.1029/2005GL023247, 2005.~~

562 ~~Vaughan, D. G., Marshall, G. J., Connolley, W. M., Parkinson, C., Mulvaney, R., Hodgson, D. A., King, J. C., Pudsey,~~
563 ~~C. J. and Turner, J.: Recent rapid regional climate warming on the Antarctic Peninsula, Clim. Change, 60(3),~~
564 ~~243–274, doi:10.1023/A:1026021217991, 2003:References~~

565 ~~Abram, N. J., Mulvaney, R., Vimeux, F., Phipps, S. J., Turner, J. and England, M. H.: Evolution of the Southern Annular~~
566 ~~Mode during the past millennium, Nat. Clim. Chang., 4(7), 564–569, doi:10.1038/nclimate2235, 2014.~~

567 ~~Adusumilli, S., Fricker, H. A., Siegfried, M. R., Padman, L., Paolo, F. S. and Ligtenberg, S. R. M.: Variable Basal Melt Rates~~
568 ~~of Antarctic Peninsula Ice Shelves, 1994–2016, Geophys. Res. Lett., 45(9), 4086–4095, doi:10.1002/2017GL076652,~~
569 ~~2018.~~

570 ~~Alley, K. E., Scambos, T. A., Miller, J. Z., Long, D. G. and MacFerrin, M.: Quantifying vulnerability of Antarctic ice shelves~~
571 ~~to hydrofracture using microwave scattering properties, Remote Sens. Environ., 210, 297–306,~~
572 ~~doi:10.1016/j.rse.2018.03.025, 2018.~~

573 ~~Banwell, A. F., Caballero, M., Arnold, N. S., Glasser, N. F., Cathles, L. Mac and MacAyeal, D. R.: Supraglacial lakes on the~~
574 ~~Larsen B ice shelf, Antarctica, and at Paakitsoq, West Greenland: A comparative study, Ann. Glaciol., 55(66), 1–8,~~
575 ~~doi:10.3189/2014AoG66A049, 2014.~~

576 ~~Banwell, A. F., MacAyeal, D. R. and Sergienko, O. V.: Breakup of the Larsen B Ice Shelf triggered by chain reaction~~
577 ~~drainage of supraglacial lakes, Geophys. Res. Lett., 40(22), 5872–5876, doi:10.1002/2013GL057694, 2013.~~

578 ~~Banwell, A. F., Willis, I. C., Macdonald, G. J., Goodsell, B. and MacAyeal, D. R.: Direct measurements of ice-shelf flexure~~
579 ~~caused by surface meltwater ponding and drainage, Nat. Commun., 10(1), doi:10.1038/s41467-019-08522-5, 2019.~~

580 ~~Banwell, A. F., Willis, I. C., MacDonald, G. J., Goodsell, B., Mayer, D. P., Powell, A. and MacAyeal, D. R.: Calving and~~
581 ~~ripping on the McMurdo Ice Shelf, Antarctica, Ann. Glaciol., 58(75), 78–87, doi:10.1017/aog.2017.12, 2017.~~

582 Bell, R. E., Banwell, A. F., Trusel, L. D. and Kingslake, J.: Antarctic surface hydrology and impacts on ice-sheet mass
583 balance, *Nat. Clim. Chang.*, 8(12), 1044–1052, doi:10.1038/s41558-018-0326-3, 2018.

584 Bevan, S. L., Luckman, A., Hubbard, B., Kulessa, B., Ashmore, D., Kuipers Munneke, P., O’Leary, M., Booth, A., Sevestre,
585 H. and McGrath, D.: Centuries of intense surface melt on Larsen C Ice Shelf, *Cryosphere*, doi:10.5194/tc-11-2743-2017,
586 2017.

587 Borstad, C., Khazendar, A., Scheuchl, B., Morlighem, M., Larour, E. and Rignot, E.: A constitutive framework for predicting
588 weakening and reduced buttressing of ice shelves based on observations of the progressive deterioration of the remnant
589 Larsen B Ice Shelf, *Geophys. Res. Lett.*, 43(5), 2027–2035, doi:10.1002/2015GL067365, 2016.

590 Bozkurt, D., Rondanelli, R., Marín, J. C. and Garreaud, R.: Foehn Event Triggered by an Atmospheric River Underlies
591 Record-Setting Temperature Along Continental Antarctica, *J. Geophys. Res. Atmos.*, doi:10.1002/2017JD027796, 2018.

592 Bozkurt, D., Bromwich, D. H., Carrasco, J., Hines, K. M., Maureira, J. C. and Rondanelli, R.: Recent Near-surface
593 Temperature Trends in the Antarctic Peninsula from Observed, Reanalysis and Regional Climate Model Data, *Adv.
594 Atmos. Sci.*, 37(5), 477–493, doi:10.1007/s00376-020-9183-x, 2020.

595 Bozkurt, D., Bromwich, D. H., Carrasco, J. and Rondanelli, R.: Temperature and precipitation projections for the Antarctic
596 Peninsula over the next two decades: contrasting global and regional climate model simulations, *Clim. Dyn.*,
597 doi:10.1007/s00382-021-05667-2, 2021.

598 Braun, M. and Humbert, A.: Recent retreat of wilkins ice shelf reveals new insights in ice shelf breakup mechanisms, *IEEE
599 Geosci. Remote Sens. Lett.*, 6(2), 263–267, doi:10.1109/LGRS.2008.2011925, 2009.

600 Burton, J. C., Cathles, L. Mac and Wilder, W. G.: The role of cooperative iceberg capsize in ice-shelf disintegration, *Ann.
601 Glaciol.*, 54(63), 84–90, doi:10.3189/2013AoG63A436, 2013.

602 Cape, M. R., Vernet, M., Skvarca, P., Marinsek, S., Scambos, T. and Domack, E.: Foehn winds link climate-driven warming
603 to ice shelf evolution in Antarctica, *J. Geophys. Res.*, doi:10.1002/2015JD023465, 2015.

604 Carrasco, J. F., Bozkurt, D. and Cordero, R. R.: A review of the observed air temperature in the Antarctic Peninsula. Did the
605 warming trend come back after the early 21st hiatus?, *Polar Sci.*, 28, doi:10.1016/j.polar.2021.100653, 2021.

606 Cook, A. J. and Vaughan, D. G.: Ice shelf changes on the Antarctic Peninsula Overview of areal changes of the ice shelves
607 on the Antarctic Peninsula over the past 50 years Ice shelf changes on the Antarctic Peninsula, *TCD*, 3, 579–630
608 [online] Available from: www.the-cryosphere-discuss.net/3/579/2009/, 2009.

609 Datta, R. T., Tedesco, M., Fettweis, X., Agosta, C., Lhermitte, S., Lenaerts, J. T. M. and Wever, N.: The Effect of
610 Foehn Induced Surface Melt on Firn Evolution Over the Northeast Antarctic Peninsula, *Geophys. Res. Lett.*,
611 2018GL080845, doi:10.1029/2018GL080845, 2019.

612 Depoorter, M. A., Bamber, J. L., Griggs, J. A., Lenaerts, J. T. M., Ligtner, S. R. M., Van Den Broeke, M. R. and Moholdt,
613 G.: Calving fluxes and basal melt rates of Antarctic ice shelves, *Nature*, 502(7469), 89–92, doi:10.1038/nature12567,
614 2013.

615 Doake, C. S. M., Corr, H. F. J., Rott, H., Skvarca, P. and Young, N. W.: Breakup and conditions for stability of the northern
616 Larsen Ice Shelf, *Antarctica*, *Nature*, 391, 778–780, 1988.

617 Elvidge, A. D., Kuipers Munneke, P., King, J. C., Renfrew, I. A. and Gilbert, E.: Atmospheric Drivers of Melt on Larsen C
618 Ice Shelf: Surface Energy Budget Regimes and the Impact of Foehn, *J. Geophys. Res. Atmos.*, 125(17),
619 doi:10.1029/2020JD032463, 2020.

620 Elvidge, A. D., Renfrew, I. A., King, J. C., Orr, A., Lachlan-Cope, T. A., Weeks, M. and Gray, S. L.: Foehn jets over the
621 Larsen C Ice Shelf, *Antarctica*, *Q. J. R. Meteorol. Soc.*, 141(688), 698–713, doi:10.1002/qj.2382, 2015.

622 Glasser, N. F. and Scambos, T. A.: A structural glaciological analysis of the 2002 Larsen B ice-shelf collapse, *J. Glaciol.*,
623 54(184), 3–16, doi:10.3189/002214308784409017, 2008.

624 Glasser, N. F., Kulesa, B., Luckman, A., Jansen, D., King, E. C., Sammonds, P. R., Scambos, T. A. and Jezek, K. C.:
625 Surface structure and stability of the Larsen C ice shelf, *Antarctic Peninsula*, 2009.

626 Grosvenor, D. P., King, J. C., Choularton, T. W. and Lachlan-Cope, T.: Downslope föhn winds over the antarctic peninsula
627 and their effect on the larsen ice shelves, *Atmos. Chem. Phys.*, 14(18), 9481–9509, doi:10.5194/acp-14-9481-2014,
628 2014.

629 Gudmundsson, G. H.: Ice-shelf buttressing and the stability of marine ice sheets, *Cryosphere*, 7(2), 647–655,
630 doi:10.5194/tc-7-647-2013, 2013. Holland, P. R., Corr, H. F. J., Pritchard, H. D., Vaughan, D. G., Arthern, R. J., Jenkins,
631 A. and Tedesco, M.: The air content of Larsen Ice Shelf, *Geophys. Res. Lett.*, doi:10.1029/2011GL047245, 2011.

632 King, J. C., Gadian, A., Kirchaessner, A., Kuipers Munneke, P., Lachlan-Cope, T. A., Orr, A., Reijmer, C., van den Broeke,
633 M. R., van Wessem, J. M. and Weeks, M.: Validation of the summertime surface energy budget of Larsen C Ice Shelf
634 (Antarctica) as represented in three high-resolution atmospheric models, *J. Geophys. Res.*, 120(4), 1335–1347,
635 doi:10.1002/2014JD022604, 2015.

636 King, J. C., Kirchaessner, A., Bevan, S., Elvidge, A. D., Kuipers Munneke, P., Luckman, A., Orr, A., Renfrew, I. A. and van
637 den Broeke, M. R.: The Impact of Föhn Winds on Surface Energy Balance During the 2010–2011 Melt Season Over
638 Larsen C Ice Shelf, *Antarctica*, *J. Geophys. Res. Atmos.*, doi:10.1002/2017JD026809, 2017.

639 Kirchaessner, A., King, J. C. and Anderson, P. S.: The Impact of Föhn Conditions Across the Antarctic Peninsula on Local
640 Meteorology Based on AWS Measurements, *J. Geophys. Res. Atmos.*, 126(4), doi:10.1029/2020JD033748, 2021.

641 Kuipers Munneke, P., Luckman, A. J., Bevan, S. L., Smeets, C. J. P. P., Gilbert, E., van den Broeke, M. R., Wang, W.,
642 Zender, C., Hubbard, B., Ashmore, D., Orr, A., King, J. C. and Kulesa, B.: Intense Winter Surface Melt on an Antarctic
643 Ice Shelf, *Geophys. Res. Lett.*, doi:10.1029/2018GL077899, 2018.

644 Kuipers Munneke, P., Van Den Broeke, M. R., King, J. C., Gray, T. and Reijmer, C. H.: Near-surface climate and surface
645 energy budget of Larsen C ice shelf, Antarctic Peninsula, *Cryosphere*, 6(2), 353–363, doi:10.5194/tc-6-353-2012, 2012.

646 Laffin, M. K., Zender, C. S., Singh, S., Van Wessem, J. M., Smeets, C. J. P. P. and Reijmer, C. H.: Climatology and
647 Evolution of the Antarctic Peninsula Föhn Wind-Induced Melt Regime From 1979–2018, *J. Geophys. Res. Atmos.*,
648 126(4), doi:10.1029/2020JD033682, 2021.

649 Larour, E., Rignot, E., Poinelli, M. and Scheuchl, B.: Physical processes controlling the rifting of Larsen C Ice Shelf,
650 Antarctica, prior to the calving of iceberg A68, *Proc. Natl. Acad. Sci. U. S. A.*, 118(40), doi:10.1073/pnas.2105080118,
651 2021.

652 Leeson, A. A., Forster, E., Rice, A., Gourmelen, N. and van Wessem, J. M.: Evolution of Supraglacial Lakes on the Larsen B
653 Ice Shelf in the Decades Before it Collapsed, *Geophys. Res. Lett.*, 47(4), doi:10.1029/2019GL085591, 2020.

654 Leeson, A. A., Van Wessem, J. M., Ligtenberg, S. R. M., Shepherd, A., Van Den Broeke, M. R., Killick, R., Skvarca, P.,
655 Marinsek, S. and Colwell, S.: Regional climate of the Larsen B embayment 1980-2014, *J. Glaciol.*, 63(240), 683–690,
656 doi:10.1017/jog.2017.39, 2017.

657 Lenaerts, J. T. M., Lhermitte, S., Drews, R., Ligtenberg, S. R. M., Berger, S., Helm, V., Smeets, C. J. P. P., Broeke, M. R. V.
658 Den, Van De Berg, W. J., Van Meijgaard, E., Eijkelboom, M., Eisen, O. and Pattyn, F.: Meltwater produced by
659 wind-albedo interaction stored in an East Antarctic ice shelf, *Nat. Clim. Chang.*, doi:10.1038/nclimate3180, 2017.

660 Lhermitte, S., Sun, S., Shuman, C., Wouters, B., Pattyn, F., Wuite, J., Berthier, E. and Nagler, T.: Damage accelerates ice
661 shelf instability and mass loss in Amundsen Sea Embayment, *Sci. Libr. Ser.*, 117,
662 doi:10.1073/pnas.1912890117/-/DCSupplemental.y, 2020.

663 Lim, E. P., Hendon, H. H., Arblaster, J. M., Delage, F., Nguyen, H., Min, S. K. and Wheeler, M. C.: The impact of the
664 Southern Annular Mode on future changes in Southern Hemisphere rainfall, *Geophys. Res. Lett.*, 43(13), 7160–7167,
665 doi:10.1002/2016GL069453, 2016.

666 Luckman, A., Elvidge, A., Jansen, D., Kulesa, B., Kuipers Munneke, P., King, J. and Barrand, N. E.: Surface melt and
667 ponding on Larsen C Ice Shelf and the impact of föhn winds, *Antarct. Sci.*, doi:10.1017/S0954102014000339, 2014.

668 Massom, R. A., Scambos, T. A., Bennetts, L. G., Reid, P., Squire, V. A. and Stammerjohn, S. E.: Antarctic ice shelf
669 disintegration triggered by sea ice loss and ocean swell, *Nature*, 558(7710), 383–389, doi:10.1038/s41586-018-0212-1,
670 2018.

671 McGrath, D., Steffen, K., Holland, P. R., Scambos, T., Rajaram, H., Abdalati, W. and Rignot, E.: The structure and effect of
672 suture zones in the Larsen C Ice Shelf, Antarctica, *J. Geophys. Res. Earth Surf.*, 119(3), 588–602,
673 doi:10.1002/2013JF002935, 2014.

674 Morris, E. M. and Vaughan, D. G.: Spatial and Temporal Variation of Surface Temperature on the Antarctic Peninsula and
675 the Limit of Viability of Ice Shelves, *Antarct. Res. Ser.*, 79, 61–68, doi:10.1029/079ARS05, 2003.

676 Mulvaney, R., Abram, N. J., Hindmarsh, R. C. A., Arrowsmith, C., Fleet, L., Triest, J., Sime, L. C., Alemany, O. and Foord,
677 S.: Recent Antarctic Peninsula warming relative to Holocene climate and ice-shelf history, *Nature*, 489(7414), 141–144,
678 doi:10.1038/nature11391, 2012.

679 Munneke, P. K., Ligtenberg, S. R. M., Van Den Broeke, M. R. and Vaughan, D. G.: Firm air depletion as a precursor of
680 Antarctic ice-shelf collapse, *J. Glaciol.*, 60(220), 205–214, doi:10.3189/2014JoG13J183, 2014.

681 Polashenski, C., Golden, K. M., Perovich, D. K., Skyllingstad, E., Arnsten, A., Stwertka, C. and Wright, N.: Percolation
682 blockage: A process that enables melt pond formation on first year Arctic sea ice, *J. Geophys. Res. Ocean.*, 122(1),
683 413–440, doi:10.1002/2016JC011994, 2017.

684 Pollard, D., DeConto, R. M. and Alley, R. B.: Potential Antarctic Ice Sheet retreat driven by hydrofracturing and ice cliff
685 failure, *Earth Planet. Sci. Lett.*, 412, 112–121, doi:10.1016/j.epsl.2014.12.035, 2015.

686 Pritchard, H. D., Ligtenberg, S. R. M., Fricker, H. A., Vaughan, D. G., Van Den Broeke, M. R. and Padman, L.: Antarctic
687 ice-sheet loss driven by basal melting of ice shelves, *Nature*, 484(7395), 502–505, doi:10.1038/nature10968, 2012.

688 Qiao, G., Li, Y., Guo, S. and Ye, W.: Evolving instability of the scar inlet ice shelf based on sequential landsat images
689 spanning 2005–2018, *Remote Sens.*, 12(1), doi:10.3390/RS12010036, 2020.

690 Rack, W. and Rott, H.: Pattern of retreat and disintegration of the Larsen B ice shelf, Antarctic Peninsula, *Ann. Glaciol.* , 39,
691 505–510 [online] Available from: <https://www.cambridge.org/core>., 2004.

692 Rignot, E., Jacobs, S., Mouginot, B. and Scheuchl, B.: Ice-Shelf Melting Around Antarctica, *Science* (80-.), 341(6143),
693 263–266, doi:10.1126/science.1237966, 2013. Rignot, E., Casassa, G., Gogineni, P., Krabill, W., Rivera, A. and Thomas,
694 R.: Accelerated ice discharge from the Antarctic Peninsula following the collapse of Larsen B ice shelf, *Geophys. Res.*
695 *Lett.*, 31(18), doi:10.1029/2004GL020697, 2004.

696 Robel, A. A. and Banwell, A. F.: A Speed Limit on Ice Shelf Collapse Through Hydrofracture, *Geophys. Res. Lett.*, 46(21),
697 12092–12100, doi:10.1029/2019GL084397, 2019. Rott, H., Rack, W., Nagler, T. and Skvarca, P.: Climatically induced
698 retreat and collapse of norther Larsen Ice Shelf, Antarctic Peninsula, *Ann. Glaciol.*, 27, 86–92,
699 doi:10.3189/s0260305500017262, 1998.

700 Sandhäger, H., Rack, W. and Jansen, D.: Model investigations of Larsen B Ice Shelf dynamics prior to the breakup. [online]
701 Available from: <http://www.uib.no/People/ngfls/frisp/Rep16/sandhageretal.pdf>, 2005.

702 Scambos, T. A., Bohlander, J. A., Shuman, C. A. and Skvarca, P.: Glacier acceleration and thinning after ice shelf collapse in
703 the Larsen B embayment, Antarctica, *Geophys. Res. Lett.*, 31(18), doi:10.1029/2004GL020670, 2004.

704 Scambos, T. A., Hulbe, C., Fahnestock, M. and Bohlander, J.: The link between climate warming and break-up of ice shelves
705 in the Antarctic Peninsula, *J. Glaciol.*, 46(154), 516–530, doi:10.3189/172756500781833043, 2000.

706 Scambos, T., Hulbe, C. and Fahnestock, M.: Climate-Induced Ice Shelf Disintegration in the Antarctic Peninsula, pp. 79–92.,
707 2003.

708 Schodlok, M. P., Menemenlis, D. and Rignot, E. J.: Ice shelf basal melt rates around Antarctica from simulations and
709 observations, *J. Geophys. Res. Ocean.*, 121(2), 1085–1109, doi:10.1002/2015JC011117, 2016.

710 Trusel, L. D., Frey, K. E., Das, S. B., Karnauskas, K. B., Kuipers Munneke, P., Van Meijgaard, E. and Van Den Broeke, M.
711 R.: Divergent trajectories of Antarctic surface melt under two twenty-first-century climate scenarios, *Nat. Geosci.*,
712 8(12), 927–932, doi:10.1038/ngeo2563, 2015.

713 Trusel, L. D., Frey, K. E., Das, S. B., Munneke, P. K. and Van Den Broeke, M. R.: Satellite-based estimates of Antarctic
714 surface meltwater fluxes, *Geophys. Res. Lett.*, 40(23), 6148–6153, doi:10.1002/2013GL058138, 2013.

715 Turton, J. V., Kirchgaessner, A., Ross, A. N. and King, J. C.: Does high-resolution modelling improve the spatial analysis of
716 föhn flow over the Larsen C Ice Shelf?, *Weather*, 72(7), doi:10.1002/wea.3028, 2017.

717 Turton, J. V., Kirchgaessner, A., Ross, A. N. and King, J. C.: The spatial distribution and temporal variability of föhn winds
718 over the Larsen C ice shelf, Antarctica, *Q. J. R. Meteorol. Soc.*, doi:10.1002/qj.3284, 2018.

719 van den Broeke, M.: Strong surface melting preceded collapse of Antarctic Peninsula ice shelf, *Geophys. Res. Lett.*, 32(12),
720 1–4, doi:10.1029/2005GL023247, 2005.

721 Vaughan, D. G., Marshall, G. J., Connolley, W. M., Parkinson, C., Mulvaney, R., Hodgson, D. A., King, J. C., Pudsey, C. J.
722 and Turner, J.: Recent rapid regional climate warming on the Antarctic Peninsula, *Clim. Change*, 60(3), 243–274,
723 doi:10.1023/A:1026021217991, 2003.

724 Wang, W., Zender, C. S., van As, D., Fausto, R. S. and Laffin, M. K.: Greenland Surface Melt Dominated by Solar and
725 Sensible Heating, *Geophys. Res. Lett.*, 48(7), doi:10.1029/2020GL090653, 2021.

726 Wiesenekker, J. M., Munneke, P. K., van den Broeke, M. R. and Paul Smeets, C. J. P.: A multidecadal analysis of Föhn
727 winds over Larsen C ice shelf from a combination of observations and modeling, *Atmosphere (Basel)*, 9(5),
728 doi:10.3390/atmos9050172, 2018.

729 Zheng, F., Li, J., Clark, R. T. and Nnamchi, H. C.: Simulation and projection of the Southern Hemisphere annular mode in
730 CMIP5 models, *J. Clim.*, 26(24), 9860–9879, doi:10.1175/JCLI-D-13-00204.1, 2013.

731